A Ferromagnetically Coupled, Bell-Shaped [Ni4Gd5] Cage

A ferromagnetically coupled, bell-shaped [Ni_4Gd_5] cage.

Foteini E. Kakaroni,[‡] Demetrios I. Tzimopoulos,[†] Hector W. L. Fraser,[§] Milosz Siczek,[∫] Tadeusz Lis,[∫] Marco Evangelisti,[#] Euan K. Brechin*[§] and Constantinos J. Milios*[‡]*

[‡]Department of Chemistry, The University of Crete, Voutes, 71003, Herakleion, Greece. E-mail: komil@uoc.gr

[†]Department of Chemistry, Aristotle University of Thessaloniki, 54124 Thessaloniki, Greece.

[§]EaStCHEM School of Chemistry, The University of Edinburgh, David Brewster Road, Edinburgh, EH9 3FJ, UK. E-mail: ebrechin@staffmail.ed.ac.uk

[∫]Department of Chemistry, University of Wroclaw, 50-283 Wroclaw, Poland.

[#]Instituto de Ciencia de Materiales de Aragón (ICMA), CSIC – Universidad de Zaragoza, 50009 Zaragoza, Spain. E-mail: evange@unizar.es

ABSTRACT

Reaction between $NiCl_2 \cdot 6H_2O$, 2-hydroxy-4-methyl-6-phenyl-pyridine-3-amidoxime (H_2L), benzoic acid and $M(NO_3)_3 \cdot 6H_2O$ (M = Gd, Y) in MeCN under basic conditions, yields the complexes $[Ni^{II}_4Gd^{III}_5(PhCOO)_{10}(HL)_4(HL_{zw})_4(OH)_2(NO_3)_2]Cl \cdot 13.6MeCN \cdot H_2O$ (**1**·13.6MeCN

·H_2O) and $[Ni^{II}_4Y^{III}_5(PhCOO)_{10}(HL)_4(HL_{zw})_4(OH)_2(NO_3)_{1.5}(H_2O)_{0.5}]0.5Cl(NO_3)\cdot 3H_2O$ (**2**·$3H_2O$). Both clusters display similar structures, consisting of a bell-shaped $\{Ni^{II}_4M^{III}_5\}$ unit, in which a linear 'zig-zag' $\{Ni_4\}$ subunit bisects the central $\{M^{III}_5\}$ 'ring'. Direct (dc) and alternating current (ac) magnetic susceptibility measurements carried out in the 2 – 300 K temperature range for complexes **1** and **2** revealed ferromagnetic intermolecular interactions, while heat-capacity measurements for the Gd analogue suggest that complex **1** lowers its temperature from $T = 9.6$ K down to 2.3 K by adiabatically demagnetizing from $B_i = 7$ T to $B_f = 0$.

KEYWORDS Polynuclear 3*d*-4*f* complexes, amidoxime ligands, magnetic properties, ferromagnetism, heat capacity.

Introduction

The field of molecular magnetism has become a multidisciplinary, dynamic field of science for which a breadth of potential applications can be envisioned. For example, anisotropic complexes "remembering" their magnetization upon removal of an initially applied magnetic field at low temperatures (< 80 K) can function as Single-Molecule Magnets (SMMs) with potential use in information storage devices.[1] Isotropic, high magnetic density cages that possess numerous field-accessible spin states have been shown to exhibit a large magnetocaloric effect that makes them excellent candidates for cryogenic refrigeration.[2] A major challenge in both areas remains the molecular design and structural control of such species, despite the fact that many, if not all, of the key ingredients are known. Indeed, synthetic control becomes increasingly more difficult as the nuclearity of the cage increases, not least when dealing with flexible organic ligands and metal ions that can display a variety of coordination geometries. Structural complexity leads to an increase in the number of intramolecular exchange pathways, and to obvious consequences for interpreting and understanding magnetic behavior. Despite these difficulties, numerous examples of such large cages exist, including an $\{Fe^{III}_{10}Gd^{III}_{10}\}$ cyclic complex with an $S = 60$ ground-state,[3] a giant $\{Fe^{III}_{18}Fe^{II}_{24}\}$ nanocluster with an $S = 45$ spin ground-state,[4] a $\{Mn^{III}_{12}Mn^{II}_{7}\}$ cluster with an $S = 83/2$ ground-state,[5] a $\{Mn^{III}_{11}Mn^{II}_{6}\}$ complex with an $S = 37$ ground-state,[6] and most recently a $[Ni_{21}Gd_{20}]$ cage displaying a remarkable (field-induced) $S = 91$ ground state.[7]

In this work, the isolation, characterization and investigation of the magnetic behavior of an enneanuclear $[Ni^{II}_{4}Gd^{III}_{5}]$ cluster are reported, built by employing the amidoxime ligand 2-hydroxy-4-methyl-6-phenyl-pyridine-3-amidoxime, H_2L (Scheme 1), which was previously employed succesfully in heterometallic chromium chemistry yielding two Cr^{III}-centered heterometallic $[M^{II}_{6}Cr^{III}]$ (M= Ni, Co) wheels.[11a] The complex

$[Ni^{II}_4Gd^{III}_5(PhCOO)_{10}(HL)_4(HL_{zw})_4(OH)_2(NO_3)_2]Cl\cdot 3.6MeCN\cdot H_2O$ (**1**·13.6MeCN·H_2O; zw = zwitter ion) displays an unusual bell-shaped[8] metal-topology, and dominant ferromagnetic intramolecular exchange interactions.

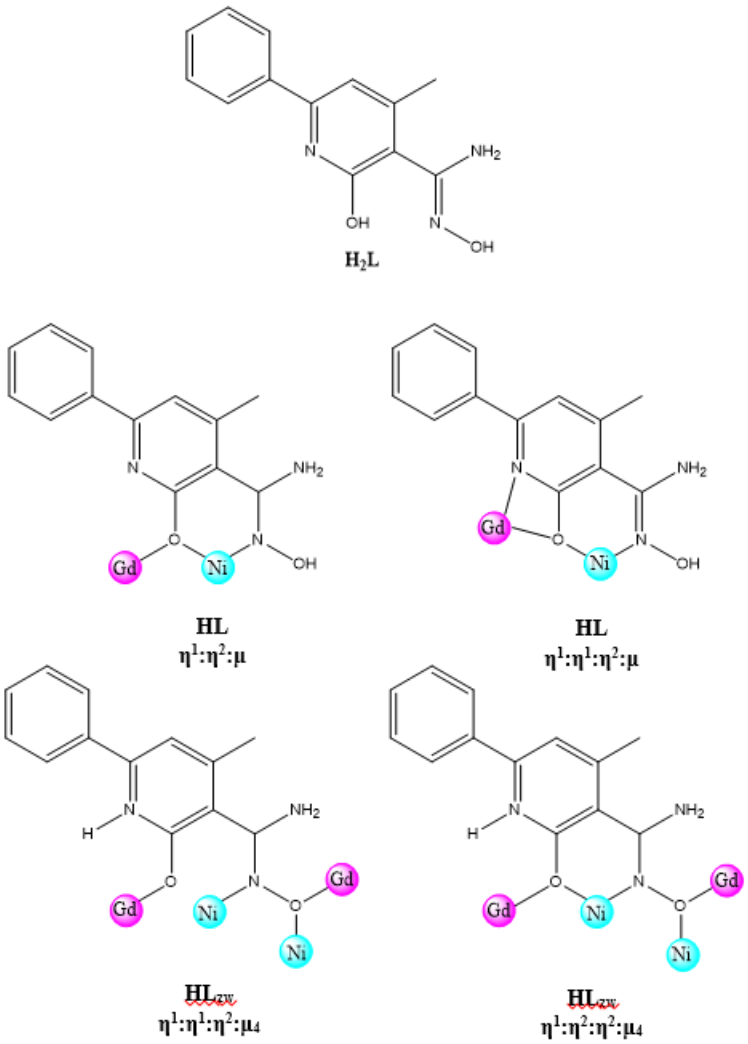

Scheme 1. The chemical structure of the ligand used in this work and its coordination modes in **1** and **2**.

Experimental Section

All synthetic procedures were performed under aerobic conditions, using materials and solvents as received.

$[Ni^{II}_4Gd^{III}_5(PhCOO)_{10}(HL)_4(HL_{zw})_4(OH)_2(NO_3)_2]Cl\cdot 13.6MeCN\cdot H_2O$ ($1\cdot 13.6MeCN\cdot H_2O$). $NiCl_2\cdot 6H_2O$ (60 mg, 0.25 mmol), $Gd(NO_3)_3\cdot 6H_2O$ (113 mg, 0.25 mmol), H_2L (122 mg, 0.5 mmol), PhCOOH (61 mg, 0.5 mmol) and NEt_3 (1.5 mmol) were added to MeCN (20 mL), and the resultant green solution left to stir for 60 minutes. The solution was then filtered and left for evaporation undisturbed at room temperature, forming yellow-green single-crystals of $\mathbf{1}\cdot 13.6MeCN\cdot H_2O$ after 2 days in ~30% yield, and collected by filtration and dried in air. Anal. calcd. for $C_{202}H_{192}ClGd_5N_{40}Ni_4O_{45}$ ($\mathbf{1}\cdot 4MeCN$): C, 48.95; H, 3.90; N, 11.30%. Found: C, 48.69; H, 3.57; N 11.16%.

$[Ni^{II}_4Y^{III}_5(PhCOO)_{10}(HL)_4(HL_{zw})_4(OH)_2(NO_3)_{1.5}(H_2O)_{0.5}]0.5Cl(NO_3)\cdot 3H_2O$ ($2\cdot 3H_2O$). Complex **2** was prepared in an analogous manner to **1**, using $Y(NO_3)_3\cdot 6H_2O$. Light-green crystals suitable for X-ray diffraction were formed after 3 days in ~25% yield. Anal. calcd. for $C_{174}H_{155}Cl_{0.5}N_{26.5}Ni_4O_{47}Y_5$ ($\mathbf{2}\cdot H_2O$): C, 52.06; H, 3.79; N, 9.25%. Found: C, 52.18; H, 3.61; N 9.13%.

Physical Methods. Elemental analyses (C, H, N) were carried out by the microanalysis service of the University of Ioannina. Solid state magnetic measurements were carried out on freshly prepared samples of **1** and **2** on a Quantum design SQUID MPMS-XL magnetometer equipped with a 7 T DC magnet at the University of Edinburgh, while the observed paramagnetic susceptibilities were corrected using Pascal's constants. Heat capacity measurements for a microcrystalline sample of complex **1** pressed into a thin pellet, were performed using a Quantum Design PPMS equipped with a ^{3}He cryostat for the temperature range (0.3 – 30) K. Apiezon-N grease was used to facilitate the thermalization of the sample at low temperatures, and its

contribution to the heat capacity was subtracted using a phenomenological expression. Powder XRD measurements on freshly prepared samples of **1** and **2** were performed on a PANalytical X'Pert Pro MPD diffractometer at the Department of Chemistry, University of Crete. FTIR–ATR (Fourier–transform infrared attenuated total reflectance) spectra were recorded on a Perkin Elmer FTIR Spectrum BX spectrometer.

X-Ray crystallography and Structure Solution.

Diffraction data for **1**·13.6MeCN ·H_2O and **2**·3H_2O were collected on an Xcalibur R four-circle diffractometer with Ruby CCD detector at 230 K and 80 K, respectively. Both structures were solved by direct methods with SHELXS [Sheldrick, G.M. A short history of SHELX *Acta Cryst*. **2008** *A64*, 112-122] program and were refined by full-matrix least-squares techniques on F2 with SHELXL [Sheldrick, G.M. Crystal structure refinement with SHELXL *Acta Cryst*. **2015** *C71*, 3-8]. All hydrogen atoms were modelled in idealized geometries as riding on their parent atoms with C–H = 0.95–0.99 Å, and with Uiso(H) = 1.2Ueq(CH, CH2) or 1.5Ueq(CH3), except for water hydrogen atoms, which were located in the Fourier maps, refined with O–H distances restrained to 0.840(1) Å and then constrained parent atoms (AFIX 3 command). Data collection parameters and structure solution and refinement details are presented in Table S2, while full crystallographic details may be found in the CIF files with CCDC reference numbers 1896818-1896819, for **1** and **2**, respectively.

Result and discussion

Synthesis. The 1: 1: 2: 2 reaction between $NiCl_2 \cdot 6H_2O$, $Gd(NO_3)_3 \cdot 6H_2O$, H_2L and benzoic acid in the presence of base, NEt_3, in MeCN gives the complex $[Ni^{II}_4Gd^{III}_5(PhCOO)_{10}(HL)_4(HL_{zw})_4(OH)_2(NO_3)_2]Cl \cdot 13.6MeCN \cdot H_2O$ (**1**$\cdot 13.6MeCN \cdot H_2O$), while upon using $Y(NO_3)_3 \cdot 6H_2O$ complex $[Ni^{II}_4Y^{III}_5(PhCOO)_{10}(HL)_4(HL_{zw})_4(OH)_2(NO_3)_{1.5}(H_2O)_{0.5}]0.5Cl(NO_3) \cdot 3H_2O$ (**2**$\cdot 3H_2O$) was isolated. The formation of the enneanuclear species **1** may be summarized in the following chemical eqn. (1):

$$4\ NiCl_2 \cdot 6H_2O + 5\ Gd(NO_3)_3 \cdot 6H_2O + 8\ H_2L + 10\ PhCOOH \longrightarrow [Ni_4Gd_5(PhCOO)_{10}(HL)_4(HL_{zw})_4(OH)_2(NO_3)_2]Cl + 13\ NO_3^- + 7\ Cl^- + 20\ H^+ + 51\ H_2O \quad (1)$$

In order to fully investigate the synthetic parameters that dictate the formation of **1** (and **2**) we performed the reaction upon employing various bases *i.e.* NMe_4OH and NaOH, and also increased the duration of the reaction, but in all cases complex **1** was the product as observed by IR spectroscopy and pXRD. In addition, upon increasing the metal:ligand ratio from 1:1:2:2 initially employed in the original reaction to 1:1:1:1 we again managed to isolate only complex **1**, *albeit* in very small yield (only a handful of crystals). Finally, we performed the reaction under solvothermal conditions, but in all cases a green-white amorphous solid was obtained.

Description of Structures. Both compounds crystallize in non-centrosymmetric space groups *Aba*2 (**1**) and $Pca2_1$ (**2**), although are not isomorphous. Both complexes possess similar structures, *albeit* the crystal data for **2** are of poorer quality than those for **1**, and so for the sake of brevity we discuss only the crystal structure of **1**. The metallic skeleton of complex **1** (Figure 1) may be

described as an enneanuclear, bell-shaped $\{Ni^{II}_4Gd^{III}_5\}$ unit, in which a linear 'zig-zag' $\{Ni_4\}$ subunit bisects a $\{Gd^{III}_5\}$ 'ring' into dinuclear and trinuclear fragments (Figure 1, bottom). The inner core consists of a planar pentametallic $\{Ni^{II}_2Gd^{III}_3\}$ fragment held in position by: i) a rare η^2: η^2: η^2: μ_5 central nitrate anion, ii) two μ_3 OH^- groups, iii) two –N-O-$_{oximate}$ and two monoatomic O_R bridges belonging to two η^2: η^2: η^1: μ_4 HL_{zw}^{-1} ligands, and iv) four η^1: η^1: μ benzoate ligands.

The external $\{Ni^{II}_2Gd^{III}_2\}$ core is held in place by two η^1: η^1: μ benzoate and two η^2: η^1: η^1: μ HL^{-1} ligands, with the link between the two fragments of the core occurring *via* two η^2: η^1: η^1: μ_4 HL_{zw}^{-1} and two η^2: η^1: μ HL^{-1} ligands. Finally, two chelating and two monodentate benzoate ligands, as well as one chelating nitrate anion, complete the coordination environment of the metal ions. All Ni^{II} centres are six-coordinate, adopting distorted octahedral geometries with bond lengths in the range, 2.02-2.11 Å. The Gd centers are eight-coordinate, adopting either square-antiprismatic (Gd1, Gd2 and symmetry equivalent) or cubic (Gd3) geometries, as defined by SHAPE analysis (Figure S1, Table S1).[9] It is noteworthy that in both structures the Ni-Ni-Ni-Ni skeleton is almost identical and the geometries of the Gd5 and Y5 ions are very similar.

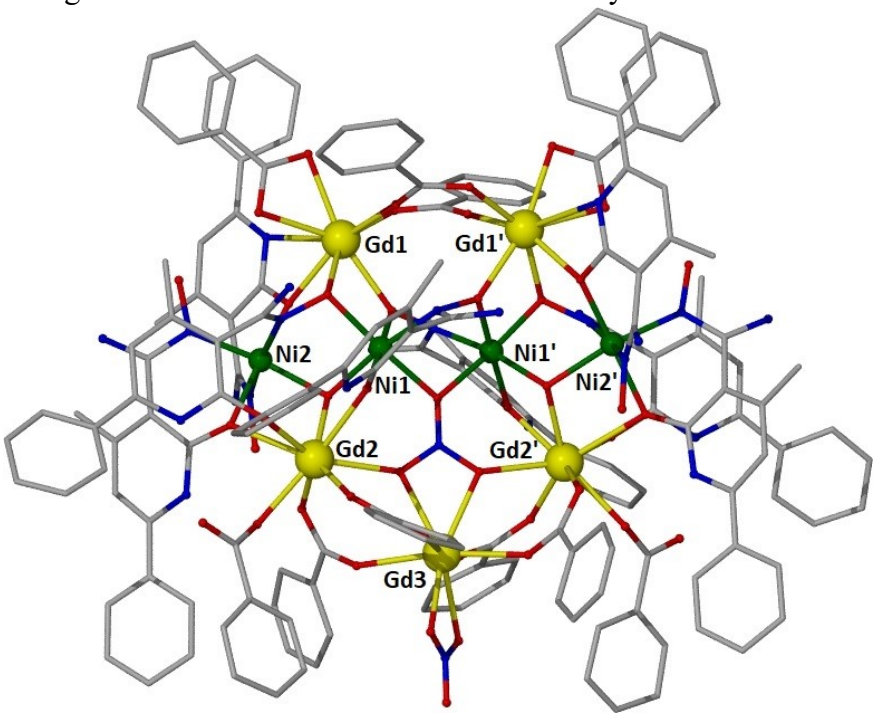

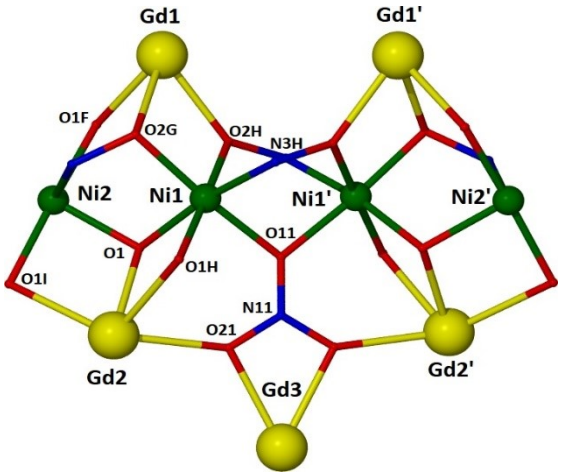

Figure 1. (Top) The molecular structure of the cation of **1**. (Bottom) The metallic skeleton of **1**. Color code: Gd^{III} = yellow, Ni^{II} = green, O = red, N = blue, C = grey. Counter-anions, solvate molecules and H-atoms have been omitted for clarity.

In the crystal lattice the molecules of **1** stack in an on-set fashion on the *b* axis with the solvate atoms located in the void space, while no significant intermolecular interactions are present (Figure S2). Again, for **2** no significant intermolecular interactions are present in the extended structure.

Magnetochemistry. The magnetic properties of **1** and **2** were investigated by DC susceptibility measurements in the 300 – 2 K temperature range under a 0.1 T applied magnetic field (Figure 2). The room-temperature $\chi_m T$ values of both complexes are very close (**1**, 46.13 $cm^3\ mol^{-1}\ K$; **2**, 4.82 $cm^3\ mol^{-1}\ K$) to the Curie constants expected for four Ni^{II} ions and five M^{III} ions (**1**, 44.21 $cm^3\ mol^{-1}\ K$; **2**, 4.84 $cm^3\ mol^{-1}\ K$), assuming $g_{Ni} = 2.2$ and $g_{Gd} = 2.0$. Upon cooling, $\chi_m T$ remains relatively constant for both complexes down to ~30/50 K (**1**/**2**) after which it rises to maximum value of 109.43/9.41 (**1**/**2**) $cm^3\ mol^{-1}\ K$. For **2**, there is a drop in $\chi_m T$ at ~5 K to a value of 8.93 $cm^3\ mol^{-1}\ K$ at 2 K. This behavior is suggestive of dominant ferromagnetic exchange between the metal centers, as confirmed by magnetization measurements (Figure 2) which saturate at 43.0 (**1**) and 8.4 (**2**) μ_B.

For **2**, we were able to simultaneously fit the magnetic susceptibility and magnetization data, using PHI[10] and employing spin-Hamiltonian (2):

$$\hat{H} = -2J_1\,\hat{s}_1\hat{s}_{1'} - 2J_2\,(\hat{s}_1\hat{s}_2 + \hat{s}_{1'}\hat{s}_{2'}) - D_1\,(\hat{s}_{1z}{}^2 + \hat{s}_{1'z}{}^2) - D_2\,(\hat{s}_{2z}{}^2 + \hat{s}_{2'z}{}^2) + g\mu_B\vec{B}\cdot(\textstyle\sum_i \vec{\hat{s}}_i) - zJ'\hat{s}_z\langle\hat{s}_z\rangle \quad (2)$$

where the J_1 exchange represents interaction between Ni1-Ni1′ mediated through one $(\text{-N-O-})_{\text{oximate}}$ bridge and one monoatomic NO_3^- bridge ($\text{Ni-O}_{\text{NO3}}\text{-Ni} \approx 102^{\text{o}}$), J_2 represents interaction between Ni1-Ni2 (and Ni1′-Ni2′) mediated by one μ_3-OH hydroxide ($\text{Ni-O}_{\text{R}}\text{-Ni} \approx 112°$) and one $(\text{-N-O-})_{\text{oximate}}$ bridge, D_1 and D_2 account for the axial single-ion zero-field splitting of Ni1 (Ni1′) and Ni2 (Ni2′) ions, respectively, and zJ' is the inter-molecular interaction. This model provided an excellent fit (Figure 2), affording the best-fit parameters $J_1 = +5.26$ (±0.09) cm^{-1}, $J_2 = +2.26$ (±0.01) cm^{-1}, $D_1 = -10.86$ (±0.10) cm^{-1}, $D_2 = 3.90$ (±0.03) cm^{-1}, $g = 2.21$ and $zJ' = 0$. The ferromagnetic nature can be attributed to the long $\text{-N}_{\text{ox}}\text{-O}_{\text{ox}}\text{-}$ bonding distances of ~1.4 Å, which have previously been reported as able to promote ferromagnetic exchange coupling in nickel oximate-based complexes.[11] Indeed, the smaller Ni1-O-Ni1′ angles would be expected to yield a stronger J_1 coupling. Remarkably, the fit reveals a change of the magnetic anisotropy, going from a stronger axial to planar symmetry, for Ni1 (Ni1′) and Ni2 (Ni2′), respectively consistent with bond lengths for Ni1 (Ni1′) up to 2.11 Å, and the lack of predominant axial symmetry in Ni2 (Ni2′). Our initial, unsuccessful, approach to fitting the magnetic data for **2** was to oversimplify the fit by imposing $J \equiv J_1 = J_2$ and $D \equiv D_1 = D_2$, *i.e.*, a 1-J + 1-D model (Figure S3). Next, we considered $D \equiv D_1 = D_2$ and different J's, *i.e.*, a 2-J + 1-D model, but the resulting fit, although slightly improved, remained unsatisfactory (Figure S4). For both models, a nonzero zJ' was needed in order to account for the

lowering of $\chi_m T$ at the low-temperature region, in contrast with the crystal structure of **2** displaying no significant intermolecular interactions.

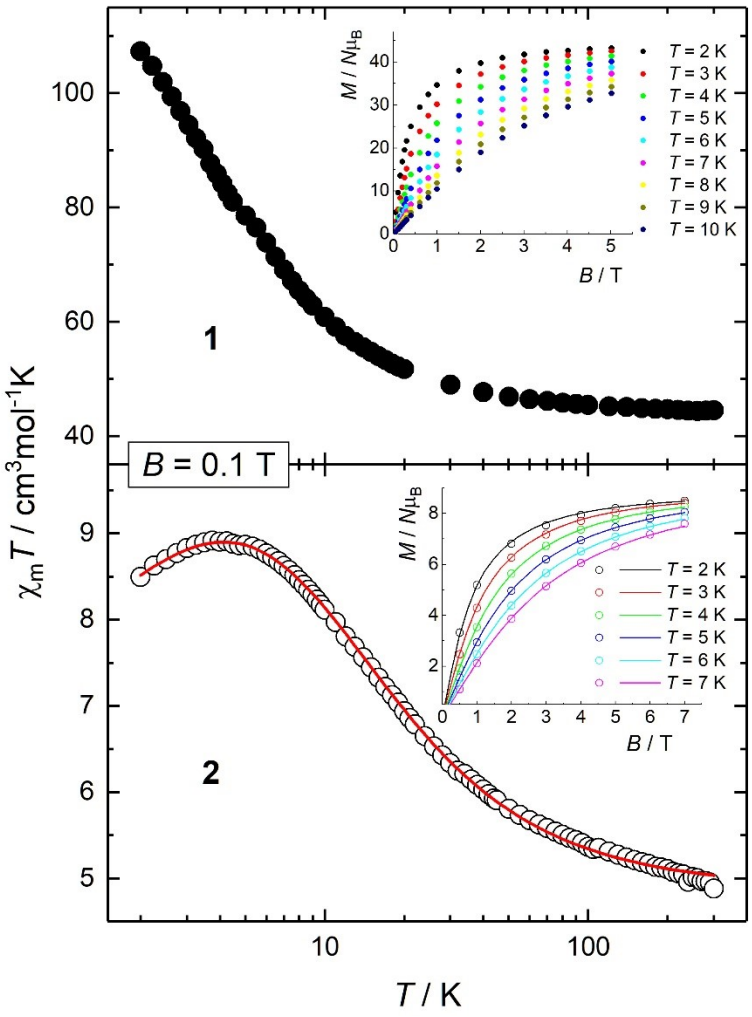

Figure 2. For **1** (top) and **2** (bottom), $\chi_m T$ *vs*. *T* plot under an 0.1 T dc field, and magnetization *M* *vs*. *B* data in the 1 – 7 T and 2.0 – 6.0 K field and temperature range (insets). The solid lines correspond to the fit of the data (see text for details).

The large ground state of Gd^{III} ($\hat{s}_{Gd}$ = 7/2), combined with the *L* = 0 angular momentum, makes **1** a potentially attractive candidate material for magnetic refrigeration.[2] Therefore, its magnetocaloric effect (MCE) was investigated, upon studying the changes of magnetic entropy,

ΔS_m, and adiabatic temperature, ΔT_{ad}, following a change of the applied magnetic field, $\Delta B = B_i - B_f$, where *i* and *f* indicate initial and final states, respectively. As heat capacity (c_p) is a powerful tool for estimating the MCE,[2] we collected temperature-dependent c_p measurements over the ~(0.3 – 30) K range under several applied magnetic fields (Figure 3). At the experimentally accessed high-temperature region, c_p may be successfully modelled upon using the Debye heat capacity, which describes the nonmagnetic lattice contribution and simplifies to a $c_{latt}/R = aT^3$ dependence at the lowest temperatures, with $a = 3.5 \times 10^{-2}$ K^{-3}, as common for molecule-based compounds. At low temperatures, c_p assumes the form of a Schottky-like anomaly that shifts to high temperature with increasing applied magnetic field. Considering that the magnetic exchange interactions between 3*d*-3*d* centres (Ni-Ni) should in principle be stronger than both the 3*d*-4*f* (Ni-Gd) and 4*f*-4*f* (Gd-Gd) interactions, the intra-molecular magnetic ordering observed at sufficiently low temperatures may be roughly described as following: four Ni^{II} centres establish a ferromagnetic net spin of $\hat{S}_{4Ni} = 4$, weakly coupled to the five peripheral Gd^{III} spins. To model the experimental data, we calculate the Schottky curves that arise from the field-split levels of the central $\hat{S}_{4Ni}$ net spin and five independent $\hat{s}_{Gd}$ spins. Then, we sum these curves to the aforementioned phonon contribution and we plot the results in Figure 3, as solid lines for $B = 1$, 3 and 7 T, respectively. The comparison with the experimental data shows that the agreement improves with increasing field value, likely because of the presence of weak but non-negligible exchange interactions involving the Gd^{III} spins, which are not taken into account in the calculations. Higher fields promote full decoupling of the weakly correlated Gd^{III} spins, yielding an excellent agreement.

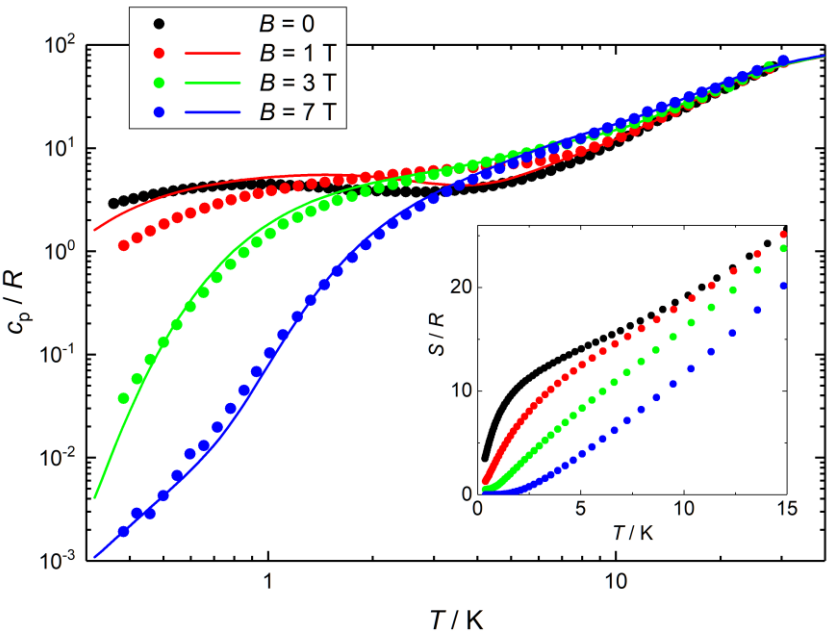

Figure 3. Heat capacity of **1**, normalized to the gas constant, c_p/R, *vs*. *T*, collected at constant field values, as labelled, in a double-log scale. For B = 1, 3 and 7 T, the solid line is the sum of the lattice (nonmagnetic) contribution and the field-split Schottky anomaly, resulting from five non-interacting $\hat{s}_{Gd}$ = 7/2 spins and a magnetically robust $\hat{S}_{4Ni}$ = 4 net spin, *i.e.*, four ferromagnetically coupled Ni^{II} spins (see text for details). (Inset) Entropy of **1**, normalized to the gas constant, S/R, *vs. T*, collected at constant field values, as labelled.

The inset of Figure 3 shows the entropy (S) that we calculate from the heat capacity data, by making use of the following equation:

$$S(T,B) = \int_0^T \frac{c_p(T',B)}{T'} dT'. \qquad (3)$$

Assuming that the Ni-Ni correlations are sufficiently strong, as to establish a ferromagnetic net spin of $\hat{S}_{4Ni}$ = 4, one would expect the magnetic entropy content to be $S_m/R = \ln(2\hat{S}_{4Ni} + 1) + 5 \times \ln(2\hat{s}_{Gd} + 1)$ = 12.6. The experimental data corroborates this assumption. As can be seen in the

inset of Figure 3, the zero-field entropy curve quickly reaches $S/R \approx 12$ at low temperatures ($T \approx$ 2.5 K). With increasing temperature, the experimental entropy gradually increases, due to the nonmagnetic lattice contribution, as expected. The maximum magnetic entropy content for 4 Ni^{II} spins ($\hat{s}_{Ni} = 1$) and 5 Gd^{III} spins ($\hat{s}_{Gd} = 7/2$) corresponds to $S_m/R = 14.8$. This value is for non-interacting spins and, therefore, cannot be reached experimentally at low temperatures.[2b]

From the entropy data, it is then straightforward to obtain the magnetocaloric effect of **1**. Figure 4 shows the results of ΔS_m and ΔT_{ad} as a function of temperature and for selected full demagnetizations, *i.e.*, $B_f = 0$. For $\Delta B = 7$ T, ΔS_m reaches 10.7 R, which is equivalent to 19.2 J kg^{-1} K^{-1}, at $T = 3.3$ K. Under the experimental conditions considered, the presence of relatively strong magnetic correlations prevents ΔS_m attaining the maximum value of magnetic entropy per mole, *i.e.*, 14.8 R. For the same value of ΔB, ΔT_{ad} reaches 7.3 K at 2.3 K, namely, the adiabatic demagnetization that starts at $T = (7.3 + 2.3)$ K = 9.6 K and $B_i = 7$ T would lower the temperature of **1** down to 2.3 K, upon reaching $B_f = 0$. With few extraordinary exceptions,[12] the Ni^{II}-Gd^{III} molecular magnetic refrigerants investigated to date possess a similar MCE, in terms of strength and temperature range, to that of **1**.[13] Besides the heat capacity, also the magnetization data can be employed for estimating ΔS_m. According to known procedures,[2b] we apply the Maxwell relation:

$$\Delta S_m(T, \Delta B) = \int_{B_i}^{B_f} \left[\frac{\partial M(T,B)}{\partial T}\right]_B dB. \qquad (4)$$

From the isothermal M *vs*. B curves of Figure 2, the so-obtained $\Delta S_m(T, \Delta B)$ values obtained for $\Delta B = 1$ and 3 T, displayed in Figure 4 (top), agree perfectly with the data obtained from c_p, thus demonstrating the robustness of the procedures employed.

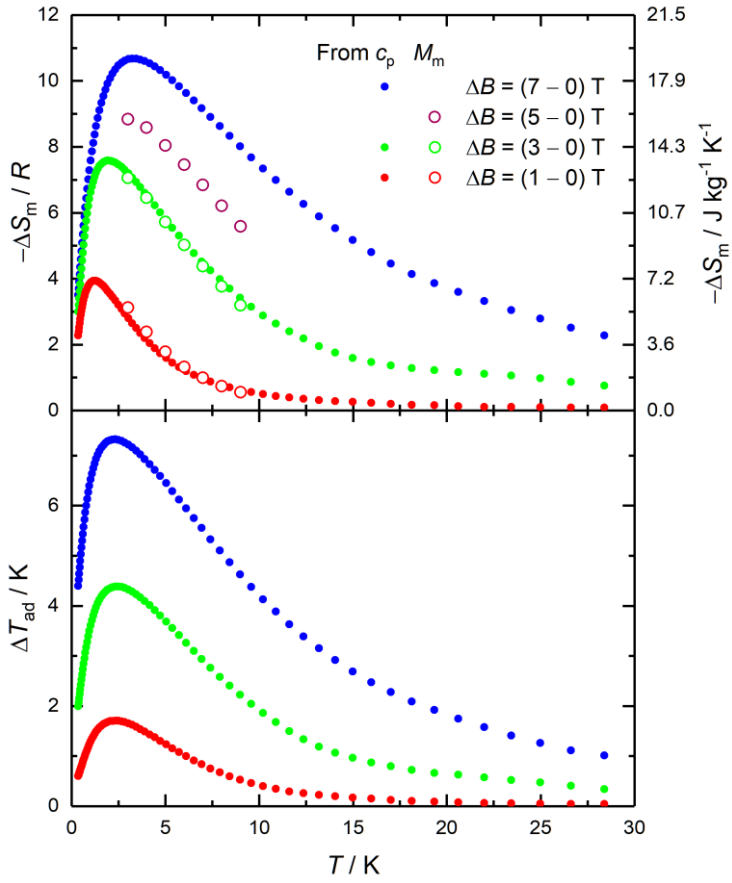

Figure 4. Magnetocaloric effect for **1**, as calculated from magnetization and heat capacity experimental data (see text for details). (Top) Magnetic entropy change, $-\Delta S_m$, normalized to the gas constant (left axis) and per unit mass (right axis), *vs*. temperature for several values of the applied magnetic field change, as labelled. (Bottom) Adiabatic temperature change, ΔT_{ad}, *vs*. temperature for several values of the applied magnetic field change, as labelled.

Conclusions

In conclusion, the use of the amidoxime ligand 2-hydroxy-4-methyl-6-phenyl-pyridine-3-amidoxime, H_2L, has led to the isolation of unusual, bell-shaped $[Ni^{II}_4M^{III}_5]$ (M = Gd (**1**), Y(**2**)) cages, in which a linear, zig-zag chain of Ni^{II} ions is sandwiched between five Gd^{III} ions. The

ligand adopts four coordination modes, bridging up to four metals. Dc magnetic susceptibility and magnetization measurements reveal the presence of dominant ferromagnetic interactions in both complexes, with analysis of the data for **2** revealing $J_{Ni\text{-}Ni}$ = 5.26 and 2.26 cm^{-1}, in accordance with previously published Ni cages containing similar structural building blocks. Magnetocaloric measurements show that complex **1** lowers its temperature from T = 9.6 K down to 2.3 K by adiabatically demagnetizing from B_i = 7 T to B_f = 0, respectively. That complex **1** is a good magnetic refrigerant at liquid helium temperatures is also manifested by the value of ΔS_m that reaches 19.2 J kg^{-1} K^{-1} at T = 3.3 K, for ΔB = 7 T.

Furthermore, our present and previously reported results[11a] on the use of the H_2L ligand strongly suggest its excellent coordination ability towards the formation of polymetallic complexes, displaying various nuclearities $\{M_x\}$ (x=7-9) and metallic topologies; thus, we are confident that further exploration of its coordination chemistry will lead to new species with beautiful structures and exciting properties.

Conflicts of interest

The authors have no conflicts to declare.

Acknowledgements

The acknowledgements come at the end of an article after the conclusions and before the notes and references.

Supporting Information Available: Crystallographic data (CIF format). This material is available free of charge via the Internet at http:// pubs.acs.org.

Corresponding Author

*C. J. Milios, komil@uoc.gr.

Funding Sources

EKB thanks the EPSRC for funding grants EP/N01331X/1 and EP/P025986/1.

Notes

REFERENCES

(1) See, for example: (a) Krylov, D. S.; Liu F.; Avdoshenko, S. M.; Spree, L.; Weise, B.; Waske, A.; Wolter, A. U. B.; Büchner, B.; Popov, A. A. Record-high thermal barrier of the relaxation of magnetization in the nitride clusterfullerene $Dy_2ScN@C_{80}$-I_h. *Chem. Commun*. **2017**, *53*, 7901-7904. (b) Liu, J.; Chen, Y.-C.; Liu, J.-L.; Vieru, V.; Ungur, L.; Jia, J.-H.; Chibotaru, L. F.; Lan, Y.; Wernsdorfer, W.; Gao, S.; Chen, X.-M.; Tong, M.-L. A Stable Pentagonal Bipyramidal Dy(III) Single-Ion Magnet with a Record Magnetization Reversal Barrier over 1000 K. *J. Am. Chem. Soc.* **2016**, *138*, 5441- 5450. (c) Ding, Y.-S.; Chilton, N. F.; Winpenny, R. E. P.; Zheng, Y.-Z. On Approaching the Limit of Molecular Magnetic Anisotropy: A Near-Perfect Pentagonal Bipyramidal Dysprosium(III) Single-Molecule Magnet. *Angew. Chem. Int. Ed.* **2016**, *55*, 16071–16074. (d) Goodwin, C. A. P.; Ortu, F.; Reta, D.; Chilton, N. F.; Mills, D. P. Molecular magnetic hysteresis at 60 kelvin in dysprosocenium. *Nature* **2017**, *548*, 439-442. (e) Guo, F.-S.; Day, B. M.; Chen, Y.-C.; Tong, M.-L.; Mansikkamäki, A.; Layfield, R. A. A Dysprosium Metallocene Single-Molecule Magnet Functioning at the Axial Limit. *Angew.Chem. Int.Ed*. **2017**, *56*, 11445-11449. (f) Guo, F.-S.; Day, B. M.; Chen, Y.-C.; Tong, M.-L.; Mansikkamäki, A.; Layfield, R. A. Magnetic hysteresis up to 80 kelvin in a dysprosium metallocene single-molecule magnet. *Science* **2018**, *362*, 1400-1403.

(2) See, for example: (a) Karotsis, G.; Evangelisti, M.; Dalgarno, S. J.; Brechin, E. K. A Calix[4]arene 3d/4f Magnetic Cooler. *Angew. Chem. Int. Ed.* **2009**, *48*, 9928-9931. (b) Evangelisti,

M.; Brechin, E. K. Recipes for enhanced molecular cooling. *Dalton Trans*. **2010**, *39*, 4672-4676. (c) Evangelisti, M.; Roubeau, O.; Palacios, E.; Camón, A.; Hooper, T. N.; Brechin, E. K.; Alonso, J. J. Cryogenic Magnetocaloric Effect in a Ferromagnetic Molecular Dimer. *Angew. Chem. Int. Ed*. **2011**, *50*, 6606-6609. (d) Martínez-Pérez, M.-J.; Montero, O.; Evangelisti, M.; Luis, F.; Sesé, J.; Cardona-Serra, S.; Coronado, E. Fragmenting Gadolinium: Mononuclear Polyoxometalate-Based Magnetic Coolers for Ultra-Low Temperatures. *Adv. Mater.* **2012**, *24*, 4301-4305. (e) Sharples, J. W.; Collison, D. Coordination compounds and the magnetocaloric effect. *Polyhedron* **2013**, *54*, 91-103. (f) Lorusso, G.; Sharples, J. W.; Palacios, E.; Roubeau, O.; Brechin, E. K.; Sessoli, R.; Rossin, A.; Tuna, F.; McInnes, E. J. L.; Collison, D.; Evangelisti, M. A Dense Metal-Organic Framework for Enhanced Magnetic Refrigeration. *Adv. Mater*. **2013**, *25*, 4653-4656. (g) Sharples, J. W.; Collison, D.; McInnes, E. J. L.; Schnack, J.; Palacios, E.; Evangelisti, M. Quantum signatures of a molecular nanomagnet in direct magnetocaloric measurements. *Nat. Commun*. **2014**, *5*, 5321-5326. (h) Pineda, E. M.; Lorusso, G.; Zangana,K. H.; Palacios, E.; Schnack, J.; Evangelisti, M.; Winpenny, R. E. P.; McInnes, E. J. L. Observation of the influence of dipolar and spin frustration effects on the magnetocaloric properties of a trigonal prismatic {Gd7} molecular nanomagnet. *Chem. Sci.* **2016**, *7*, 4891–4895.

(3) Baniodeh, A.; Magnani, N.; Lan, Y.; Buth, G.; Anson, C. E.; Richter, J.; Affronte, M.; Schnack, J.; Powell, A. K. High spin cycles: topping the spin record for a single molecule verging on quantum criticality. *npj Quantum Materials*, 2018, **3**, 10.

(4) Kang, S.; Zheng, H.; Liu, T.; Hamachi, K.; Kanegawa, S.; Sugimoto, K.; Shiota, Y.; Hayami, S.; Mito, M.; Nakamura, T.; Nakano, M.; Baker, M. L.; Nojiri, H.; Yoshizawa, K.; Duan, C.; Sato, O. A ferromagnetically coupled Fe_{42} cyanide-bridged nanocage. *Nat. Commun*. **2015**, *6*, 5955-5961.

(5) Ako, A. M.; Hewitt, I. J.; Mereacre, V.; Clérac, R.; Wernsdorfer, W.; Anson, C. E.; Powell, A. K. A Ferromagnetically Coupled Mn_{19} Aggregate with a Record S=83/2 Ground Spin State. *Angew. Chem. Int. Ed*. **2006**, *45*, 4926-4929.

(6) Moushi, E. E.; Stamatatos, T. C.; Wernsdorfer, W.; Nastopoulos, V.; Christou, G.; Tasiopoulos, A. J. A Mn_{17} Octahedron with a Giant Ground-State Spin: Occurrence in Discrete Form and as Multidimensional Coordination Polymers. *Inorg. Chem.* **2009**, *48*, 5049-5051.

(7) Chen, W.-P.; Singleton, J.; Qin, L.; Camón, A.; Engelhardt, L.; Luis, F.; Winpenny, R. E. P.; Zheng, Y.-Z. Quantum Monte Carlo simulations of a giant $\{Ni_{21}Gd_{20}\}$ cage with a $S = 91$ spin ground state. *Nat. Commun.* **2018**, *9*, 2107-2112.

(8) Mereacre, V. M.; Ako, A. M.; Clérac, R.; Wernsdorfer, W.; Filoti, G.; Bartolomé, J.; Anson, C. E.; Powell, A. K. A Bell-Shaped $Mn_{11}Gd_2$ Single-Molecule Magnet. *J. Am. Chem. Soc*. **2007**, *129,* 9248-9249.

(9) Llunell, M.; Casanova, D.; Girera, J.; Alemany, P.; Alvarez, S. SHAPE, version 2.0, Barcelona, Spain **2010**.

(10) Chilton, N. F.; Anderson, R. P.; Turner, L. D.; Soncini, A.; Murray, K. S. PHI: A powerful new program for the analysis of anisotropic monomeric and exchange-coupled polynucleard- andf-block complexes. *J. Comput. Chem*. **2013**, *34*, 1164-1175.

(11) (a) Kakaroni, F. E.; Collet, A.; Sakellari, E.; Tzimopoulos, D. I.; Siczek, M.; Lis, T.; Murrie, M.; Milios, C. J. Constructing Cr^{III}-centered heterometallic complexes: $[Ni^{II}_6Cr^{III}]$ and $[Co^{II}_6Cr^{III}]$ wheels. *Dalton Trans*. **2018**, *47*, 58-61. (b) An, G.-Y.; Wang, H.-B.; Cui, A.-L.; Kou, H.-Z. Ferromagnetic versus antiferromagnetic exchange in oximato-bridged nickel(ii) complexes. *New*

J. Chem. **2014**, *38*, 5037-5042. (c) Kou, H.-Z.; An, G.-Y.; Ji, C.-M.; Wang, B.-W.; Cui, A.-L. Ferromagnetic coupling in oximato-bridged multi-decker Ni^{II} clusters. *Dalton Trans*. **2010**, *39*, 9604-9610. (d) An, G.-Y.; Ji, C.-M.; Cui, A.-L.; Kou, H.-Z. Pyrazine-2-amidoxime Ni(II) Complexes: From Ferromagnetic Cluster to Antiferromagnetic Layer. *Inorg. Chem.* **2011**, *50*, 1079-1083. (e) Ji, C.-M.; Yang, H. –J.; Zhao, C.-C.; Tangoulis, V.; Cui, A.-L.; Kou, H.-Z. Self-Assembly of Multidecker Ni^{II} Clusters from Preformed Ni_4 Decks. *Cryst. Growth Des*. **2009**, *9,* 4607-4609.

12) (a) Peng, J.-B.; Zhang, Q.-C.; Kong, X.-J.; Ren, Y.-P.; Long, L.-S.; Huang, R.-B.; Zheng, L.-S.; Zheng, Z. A 48-Metal Cluster Exhibiting a Large Magnetocaloric Effect. *Angew. Chem. Int. Ed.* **2011**, *50*, 10649-10652. (b) Zheng, Y.-Z.; Evangelisti, M.; Winpenny, R. E. P. Large Magnetocaloric Effect in a Wells-Dawson Type $\{Ni_6Gd_6P_6\}$ Cage. *Angew. Chem. Int. Ed.* **2011**, *50*, 3692-3695. (c) Zhang, S.; Cheng, P. Magnetocaloric Effect of Two Isostructural Heterometallic Organic Frameworks Based on $\{M^{II}Gd^{III}_2\}$ Clusters (M^{II} =Mn, Ni). *ChemPlusChem* **2016**, *81*, 811-816.

13) (a) Hosoi, A.; Yukawa, Y.; Igarashi, S.; Teat, S. J.; Roubeau, O.; Evangelisti, M.; Cremades, E.; Ruiz, E.; Barrios, L. A.; Aromí, G. A Molecular Pair of $[GdNi_3]$ Tetrahedra Bridged by Water Molecules. *Chem.-Eur. J.* **2011**, *17*, 8264-8268. (b) Hooper, T. N.; Schnack, J.; Piligkos, S.; Evangelisti, M.; Brechin, E. K. The Importance of Being Exchanged: $[Gd^{III}_4M^{II}_8(OH)_8(L)_8(O_2CR)_8]^{4+}$ Clusters for Magnetic Refrigeration *Angew. Chem. Int. Ed.* **2012**, *51*, 4633-4636. (c) Pasatoiu, T. D.; Ghirri, A.; Madalan, A. M.; Affronte, M.; Andruh, M. Octanuclear $[Ni^{II}_4Ln^{III}_4]$ complexes. Synthesis, crystal structures and magnetocaloric properties *Dalton Trans.* **2014**, *43*, 9136-9142. (d) Hooper, T. N.; Inglis, R.; Lorusso, G.; Ujma, J.; Barran, P. E.; Uhrin, D.; Schnack, J.; Piligkos, S.; Evangelisti, M.; Brechin, E. K. Structurally Flexible and

Solution Stable $[Ln_4TM_8(OH)_8(L)_8(O_2CR)_8(MeOH)_y](ClO_4)_4$: A Playground for Magnetic Refrigeration. *Inorg. Chem.* **2016**, *55*, 10535-10546. (e) Guarda, E.; Bader, K.; van Slageren, J.; Alborés, P. $\{Ni^{II}_8Ln^{III}_6\}$ (Ln = Gd, Dy) rod-like nano-sized heteronuclear coordination clusters with a double carbonate bridge skeleton and remarkable MCE behavior. *Dalton Trans.* **2016**, *45*, 8566-8572. (f) Canaj, A. B; Siczek, M.; Lis, T.; Inglis, R.; Lorusso, G.; Evangelisti, M.; Milios, C. J. Tetradecanuclearity in 3d–4f chemistry: relaxation and magnetocaloric effects in $[Ni^{II}_6Ln^{III}_8]$ species. *Dalton Trans.* **2017**, *46*, 3449-3452. (g) Griffiths, K.; Harding, C.; Dokorou, V. N.; Loukopoulos, E.; Sampani, S. I.; Abdul-Sada, A.; Tizzard, G. J.; Coles, S. J.; Lorusso, G.; Evangelisti, M.; Escuer, A.; Kostakis, G. E. Heptanuclear Disk-Like $M^{II}_3Ln^{III}_4$ (M = Ni, Co) Coordination Clusters: Synthesis, Structures and Magnetic Properties. *Eur. J. Inorg. Chem.* **2017**, *33*, 3938-3945. (h) Costes, J.-P.; Dahan, F.; Vendier, L.; Shova, S.; Lorusso, G.; Evangelisti, M. Ni^{II}–Ln^{III} complexes with o-vanillin as the main ligand: syntheses, structures, magnetic and magnetocaloric properties. *Dalton Trans.* **2018**, *47*, 1106-1116.

For the Table of Contents Only

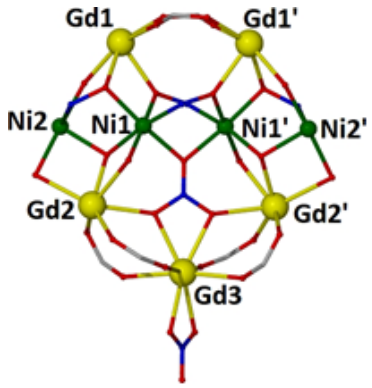

SYNOPSIS. The use of 2-hydroxy-4-methyl-6-phenyl-pyridine-3-amidoxime in Ni^{II}/M^{III} (M = Gd, Y) chemistry has provided access to two new enneanuclear $\{Ni^{II}_4M^{III}_5\}$ complexes which display dominant ferromagnetic exchange interactions.